Electrical Power and Energy Systems 118 (2020) 105738

Contents lists available at ScienceDirect

Electrical Power and Energy Systems

journal homepage: www.elsevier.com/locate/ijepes

Bi-level planning for integrated electricity and natural gas systems with wind power and natural gas storage

Xu Wang, Zhaohong Bie*, Fan Liu, Yu Kou, Lizhou Jiang

State Key Laboratory of Electrical Insulation and Power Equipment, Xi'an, China
Smart Grid Key Laboratory of Shaanxi Province, Xi'an, China
Xi'an Jiaotong University, Xi'an, China

ARTICLE INFO

Keywords:
Bi-level planning
Integrated electricity and natural gas system
Selected scenarios
Wind power
Natural gas storage
Benders decomposition

ABSTRACT

Power-to-gas facilities (PtG) are able to convert excess renewable energy into synthetic natural gas that can be stored in natural gas storage units. The coordinated planning of gas-fired generators, PtG and natural gas storage offers the prospect of mitigating energy shortages and accommodating renewable energy within integrated electricity and natural gas systems (IEGS). This paper presents a bi-level planning model for IEGS that minimizes the investment costs of candidate assets, especially wind farms, PtG facilites and natural gas storage units, as well as the operational cost over the planning horizon. A small number of carefully selected scenarios are presented to illustrate the uncertainty of wind power. IEGS operation is also analyzed on the basis of these temporal scenarios, including the operational characteristics and constraints of two systems to assess the potential role of natural gas storage and PtG. The proposed model is a scenario-based planning model that is solved by a bi-level iterative algorithm. The upper-level base-scenario based planning problem determines the candidate assets while the lower-level problem checks the feasibility using the determined components for other scenarios. Two sets of numerical tests are presented to demonstrate the effectiveness of the proposed planning model and associated algorithms.

1. Introduction

Due to their high efficiency, flexible responsiveness and lower carbon emissions, the number of gas-fired generators and their capacity has been steadily increasing. In China, it is predicted that the power output of gas-fired generators will increase to 28,500 BWh in 2020, which will make up 7% of China's total electricity production [1]. With the growth in the capacity of gas-fired generators, the proportion of gas consumed to generate electricity in China increased from 16% in 2012 to 19.9% in 2017. Meanwhile, the capacity of renewable energy had reached 36.6% of China's overall generator capacity in 2017 [2]. As power-to-gas conversion (PtG) can convert excess renewable energy into synthetic natural gas [3–5], it is widely regarded as a promising technology for renewable energy integration. On the one hand, gas system operators have been required to install more pipelines to meet the rapid growth in demand from gas-fired generators. On the other hand, the installation of PtG should also consider connection to the gas system for the injection and transportation of synthetic gas. Therefore, gas-fired generators and PtG link the electricity system and natural gas system tightly as one integrated energy system. Comprehensive expansion planning strategies are required to ensure the secure and economic operation of integrated electricity and natural gas system (IEGS). Since energy supply is critical to development, the planning of IEGS is already supervised by government departments [6,7] and carried out by regional energy companies [8,9].

The planning of IEGS has been approached from a combined operational and investment perspective to determine the type, capacity, location and time of candidate components over the planning horizon. As the accurate modeling of components is foundational to the building of optimal energy networks, in [10,11], the components were modeled in terms of energy supply, energy transportation and energy use. Not only hydro plants, wind farms, thermal generators and transmission lines, but natural gas wells, pipelines, compressors, liquefied natural gas terminals and gas storage were incorporated into this planning model. Steady-state gas flow is generally described by the Weymouth equation, which is nonlinear and nonconvex. To make the planning problem tractable, [10,12–15] have all employed a simplified transportation model without considering nodal pressure. In [16], the Weymouth equation was linearized by using a first-order Taylor series approximation and the approximations were then handled by the

* Corresponding author.
E-mail address: zhbie@mail.xjtu.edu.cn (Z. Bie).

https://doi.org/10.1016/j.ijepes.2019.105738
Received 31 July 2019; Received in revised form 20 October 2019; Accepted 24 November 2019
Available online 11 December 2019

Nomenclature

Sets and Indexes

b, t, h	index of load duration cure/hours/planning year
i, j, a	index of generators/wind farms/PtG facilities
k, p, d	index of gas storage/gas pipelines/gas load
l, m, e	index of transmission lines/buses/electrical load
o, q	index of optimality cut/feasibility cut
r, N_p	index, number of piecewise linearization segments
s, n, c	index of gas wells/gas nodes/gas compressors
CA, CS	set of candidate PtG facilities/gas storage
CL, CP	set of candidate transmission lines/gas pipelines
CG, CW	set of candidate generators/wind farms
EG, GU	set of existing generators/gas-fired generators
EL, PB	set of existing transmission lines/electrical buses
EP, GC	set of existing gas pipelines/gas compressors
$E(m), G(n)$	set of components at electric bus m/gas node n
GS, GN, T	set of gas wells/gas nodes, operating hours
ω, Ω	index, set of the wind power scenarios

Variables

CU_q^F	feasibility cut of lower-level problems of rank q
$F_{s,t,b}^{\omega,h}$, $\pi_{n,t,b}^{\omega,h}$	gas production of gas well S/Nodal pressure of gas node n of scenario ω at hour t of b load in year h
$F_{c,t,b}^{\omega,h}$, $\tau_{c,t,b}^{\omega,h}$	gas flow/gas consumption of compressor c of scenario ω at hour t of b load in year h
$F_{p,t,b}^{\omega,h}$, $S_{k,t,b}^{\omega,h}$	gas flow in pipeline p/gas stored in gas storage k of scenario ω at hour t of b load in year h
$F_{i,t,b}^{\omega,h}$, $F_{a,t,b}^{\omega,h}$	gas consumed by generator i/gas production of PtG a of scenario ω at hour t of b load in year h
IC, OC	Investment cost/operation cost
OC_o^{Sum}, CU_o^O	accumulated operation cost/optimality cut of lower-level problem of rank o
$P_{i,t,b}^{\omega,h}$, $P_{j,t,b}^{\omega,h}$	dispatch power of generator i/wind farm j of scenario ω at hour t of b load in year h
$P_{a,t,b}^{\omega,h}$, $P_{l,t,b}^{\omega,h}$	power consumption of PtG a/power flow of transmission l of scenario ω at hour t of b load in year h
$Q_{k,t,b}^{\omega,h}$, $D_{k,t,b}^{\omega,h}$	gas charging rate/discharging rate of gas storage k of scenario ω at hour t of b load in year h
y_i^h, y_j^h, y_l^h	investment status of generator i/wind farm j/transmission line l in year h
z_a^h, z_k^h, z_p^h	investment status of PtG a/gas storage k/pipeline p in year h
$\theta_{m,t,b}^{\omega,h}$	phase angle of bus m of scenario ω at hour t of b load in year h
$\delta_{p,t,b}^{r,\omega,h}$, $\varsigma_{p,t,b}^{r,\omega,h}$	continuous variables/ binary variables to indicate the segment of piecewise linearization of pipeline p of scenario ω at hour t of b load in year h

Constants and Functions

$B_{l(mn)}$, C_{mn}	susceptance of transmission mn/Weymouth coefficient of pipeline mn
C^{inv}	investment cost of a candidate electricity/gas asset
C_i^{fuel}, C_s^{gas}	fuel cost of coal-fired generator i/production cost of gas well s
C_k^{ope}, C_i^{EM}	operation cost of gas storage k/carbon emission cost of generator i
$F_p^{(r)}$, $S_{k,0}$	value of Gas flow at segment r of pipeline p/initial gas stored in gas storage k
$P_{j,t}^{BS(f)}$	forecast wind power from historical date of wind farm j at hour t
$P_{e,t,b}^h$, $F_{d,t,b}^h$	forecast electrical load e/gas load d at time t of b load in year h
P^{RU}, P^{RD}	up/down ramping limit of unit
R_b^h	system spinning reserve rate of b load in year h
ρ_ω^W, ρ_b^L	weight of wind power scenario ω/load curve b
χ, GHV	energy conversion factor/high heating value
η_k^c, η_k^d	charging/discharging rate of gas storage k
$\cdot(l)$, $\cdot(p)$	electrical bus connecting transmission line l/gas node connecting pipeline p
$(\cdot)^{\min/\max}$	Min/Max value of a quantity

Newton-Raphson method. Using the piecewise linear method introduced in [17], the planning problem of IEGS has also been transformed into mixed-integer linear programming (MILP) [18–20]. Several metaheuristic optimization methods have also been used to solve the mixed-integer nonlinear programming (MINLP) planning problem directly. These include genetic algorithms, as in [21,22], and particle swarm optimization, as in [23,24].

In terms of operational planning, the modeling of uncertainties and solution of the resulting planning model is quite challenging. In [14,15], the stochastic load demand was described by setting up various operational scenarios, leading in turn to a scenario-based planning model of IEGS. Scenario tree and corresponding scenario reduction techniques were adopted to model the load demand in a multi-stage stochastic planning model in [13,19]. Meanwhile, Monte-Carlo simulation was employed by [23–27] to sample the load scenarios more randomly. In [18,22], a contingency matrix was introduced to transform uncertain outage components into deterministic N-1 contingency scenarios in a planning model. Uncertain factors have also been broadly described as a box set with a budge constraint in the robust planning model presented in [20,28].

As decomposition and iterative algorithms offer an efficient way of solving large-scale complicated problems, they have been widely used to solve planning models when confronted with uncertain factors. In [12,20], a probabilistic reliability criterion was incorporated into IEGS planning by using Benders Decomposition. An evaluation of the system's adequacy was taken into account in the metaheuristic iterative framework in [21,24]. A two stage chance-constrained algorithm was employed in [27] to minimize the investment of candidate IEGS assets required to meet the desired confidence levels associated with energy demands. A column-and-constraint generation framework has also been used to manage the set of uncertainties in robust planning models of IEGS, such as in [20,28].

Energy storage is usually utilized to improve system operation flexibility and facilitate the integration of renewable energy [29,30]. Natural gas storage is appealing in IEGS because a large amount of gas is easier to store than electricity. The operational characteristics of natural gas storage have been discussed in [10,11]. Ref. [27] presented a planning model of IEGS with natural gas storage and assessed its value in meeting uncertain energy demands. In [31], distributed natural gas storage was included to smooth out demand curves under normal conditions and as back-up during contingencies. The potential of PtG combined with natural gas storage for storing seasonal renewable energy has also been modeled and assessed in [32].

Most research focuses on either coordinated operation and planning of PtG when accommodating wind power, or the role of natural gas storage in meeting uncertain energy demand in IEGS. However, very few papers pay attention to the possibilities of PtG and gas storage for alleviating issues arising from natural gas shortage. There is a comparative lack of natural gas as a resource in China. 20–30% of the natural gas consumed in China has to be imported every year [2]. Thus, there is a strong need for a planning model that can assess the potential of PtG and natural gas storage in China's IEGS. The purpose of this paper is to formulate an expansion planning model of IEGS that incorporates wind power and natural gas storage. From the viewpoint of

supervising government departments, this paper offers a way of minimizing the total investment in IEGS as well as the operational cost over the planning horizon. Outside of the candidate components generally considered, including coal/gas-fired generators, transmission lines, pipelines and wind farms, PtG and natural gas storage are also considered as investment candidates because of their scope for accommodating wind power and mitigating energy supply shortage.

According to the above literature, scenario-based stochastic planning models and robust optimization (RO) models offer the best ways of constructing planning models considering uncertainty. In RO models, the solutions obtained can be somewhat conservative in how they handle worst case scenarios [33]. RO-based solutions also sometimes fail to identify the infeasibility of some anticipative constraints [34]. When it comes to scenario-based optimization models, the main challenges include: (1) information about the probability of uncertain factors needs to be gathered in advance to generate representative scenarios [35]; (2) the number of scenarios can lead to them needing to be carefully merged or reduced to be able to properly balance solution accuracy and efficiency [36]. The scenario generation method proposed in [34] is effective at addressing the above concerns regarding scenario-based optimization. It involves the construction of a set of limited and carefully selected scenarios. Two special scenarios are introduced to guarantee the solution is feasible for all possible uncertainties. This scenarios generation method is therefore adopted in this paper to formulate a scenario-based stochastic planning model of IEGS with wind power. According to the different characteristics of wind power, the generated wind power scenarios can be classified into three categories: base scenarios (BS); selected vertex scenarios (SVS); and extreme ramping scenarios (ERS). BS represents normal wind power conditions, while SVS stands for the possible combination of wind power-related vertex uncertainty sets that reflect the uncertainty of wind power. ERS is specially formulated to guarantee supply in unanticipated circumstances.

With linearizing nonlinear and nonconvex Weymouth equation by incremental piecewise linearization method [17], the planning model is reformulated into an MILP problem. Though the number of scenarios is limited, the planning model remains a large-scale MILP problem because of the number of lots of auxiliary binary variables. To address the computational challenge, a bi-level iterative process based on Benders Decomposition is employed to solve the proposed planning model efficiently. In the upper-level, a deterministic planning model based on BS operational constraints is solved to optimize the investment plan. In the lower-level, the solution identified in the upper-level is checked for its feasibility and optimality by operational problems based on SVS and ERS. The stochasticity of wind power is incorporated into the planning model by testing the planned solution against SVS and ERS based operational problems.

The main contributions of this paper can be summarized as follows.

- The proposed planning model of IEGS not only considers coal/gas-fired generators, wind farms, transmission lines and pipelines as investment candidates, but also incorporates PtG and natural gas storage as candidate components for accommodating the uncertain wind power and alleviating energy supply shortages. A time-series operational model is employed to better capture the temporal correlation of wind power and effects of natural gas storage.
- A scenario-based planning model of IEGS is proposed that is based on limited and carefully selected scenarios generated using the approach outlined in [34]. With piecewise linearized Weymouth equation, the planning model is reformulated into a large-scale MILP problem. Since the scenarios of wind power are classified into three independent categories, a bi-level iterative process based on Benders Decomposition is employed to solve the planning problem efficiently. BS-based upper-level problem optimally determines appropriate candidates, while lower-level problems accommodate the stochastic character of wind power by testing the upper-level solutions against SVS and ERS-based operational problems.

The rest of the paper is organized as follows: The construction of the wind power scenarios is described in Section 2. The formulation of the proposed bi-level planning model of IEGS is presented in Section 3 and the methods that can be addressed to its solution are presented in Section 4. In Section 5, numerical cases are analyzed to assess the model's feasibility and Section 6 presents the paper's main contributions.

2. Construction of the wind power scenarios

The integration of large-scale uncertain wind power in an IEGS requires the stochastic formulation of planning model of IEGS. Scenario-based stochastic planning is a popular method for modeling the uncertainty of wind power. The core idea is to search for a finite number of scenarios that can represent all possible stochastic realizations of wind power output. On the basis of this, BS, SVS and ERS-type scenarios can be used to represent all kinds of possible wind power output [34]. BS is used to generate a standard set of scenarios to cover the uncertainty present in normal conditions. SVS is used to cover scenarios from the total minimum available wind power to the total maximum available wind power, capturing its stochasticity. ERS is formulated specifically to allow for extreme ramping scenarios when IEGS is confronted with operational problems.

2.1. Base scenarios

A base scenario represents the normal operating conditions or expected state of wind power. It is usually generated from historical or predicted data. The BS is important, as it is used to generate the box uncertainty set for the SVS. In this paper, the forecasted wind power generated from historical data is considered as the BS. It can be derived using the following:

$$P_W^{BS} = [P_{j,t}^{BS(f)}]_{K\times T}, \quad j \in CW, t \in T \tag{1}$$

2.2. Selected vertex scenarios

A polyhedral convex uncertainty set is used to represent the uncertainty of wind power and the box uncertainty set is generated by using the wind power from the BS as the mean value. The generated interval $v_{j,t} = [P_{j,t}^{\min}, P_{j,t}^{\max}]$ stands for the wind power uncertainty. SVSs are carefully selected by combining the vertices of uncertainty set. Supposing that there are K wind farms, a K-dimensional set, U_t can be used to represent the uncertainty set at time t, as in Eq. (2) with there being $N_W = 2^K$ vertices of U_t. The set of vertices V_t is denoted as shown in Eq. (3), where each vertex $v_{n,t}$ is a K-dimensional vector.

$$U_t = \{(P_{1,t}, P_{2,t}, \cdots, P_{K,t})^T | P_{j,t}^{\min} \leqslant P_{j,t} \leqslant P_{j,t}^{\max}, j \in CW, t \in T\} \tag{2}$$

$$V_t = \{v_{1,t}, v_{2,t}, \cdots, v_{N_W,t} | v_{n,t} = (P_{1,t}^n, P_{2,t}^n, \cdots, P_{K,t}^n)^T\} \tag{3}$$

To generate the SVS, the K elements in each $v_{n,t}$ are re-indexed as the total wind power output in an ascending order, as per Eq. (4). Thus, there are N_W SVSs, with the *nth* SVS is being denoted as shown in Eq. (5).

$$\sum_{j=1}^{K} \widetilde{P}_{j,t}^1 \leqslant \sum_{j=1}^{K} \widetilde{P}_{j,t}^2 \leqslant \cdots \leqslant \sum_{j=1}^{K} \widetilde{P}_{j,t}^{N_W} \tag{4}$$

$$P_W^{SVS,n} = [\widetilde{P}_{j,t}^{SVS,n}]_{K\times T}, n = 1, \cdots, N_W, j \in CW, t \in T \tag{5}$$

The uncertainty set of the wind power for each period is assumed to be the Cartesian product indicated by Eq. (6), so as to ensure that, whenever the N_W elements in each V_t are re-indexed, they are still in U_t. Meanwhile, the resulting Cartesian products are still in U. The vertices

of U are also a product of U_t. 2^K SVSs are generated as above, to cover all possible combinations of vertices for K wind farms, from the total minimum available wind power to the total maximum wind power. More detailed information about the construction of SVSs can be found in [34].

$$U = U_1 \times U_2 \times \cdots \times U_T \tag{6}$$

$$V_U = V_1 \times V_2 \times \cdots \times V_T \tag{7}$$

In this paper, just wind power is considered to illustrate the construction of scenarios relating to uncertain factors. However, this can be generalized to other uncertain factors such as load fluctuation or solar power. As the scenario construction steps for solar power are similar to those for wind power, solar power is not considered because of the limited availability of valid data.

2.3. Extreme ramping scenarios

Though SVSs cover the worst case scenarios in which all wind power is at its lowest bounds, ramping scenarios for wind farms are not fully considered. So, to cover operational problems in the model, two ERSs shown in Eqs. (8)–(9) are used to add extreme ramping scenarios. One called "OS", consists of the maximum available wind power at odd periods and minimum available wind power at even periods. The other, labeled "ES", covers the maximum available wind power at even periods and minimum available wind power at odd periods.

$$P_W^{OS} = \begin{bmatrix} P_{j,t}^{\max}, & t = 2 * \Delta t + 1 \\ P_{j,t}^{\min}, & t = 2 * \Delta t \end{bmatrix}_{K \times T}, j \in CW \tag{8}$$

$$P_W^{ES} = \begin{bmatrix} P_{j,t}^{\max}, & t = 2 * \Delta t \\ P_{j,t}^{\min}, & t = 2 * \Delta t + 1 \end{bmatrix}_{K \times T}, j \in CW \tag{9}$$

3. Formulation of bi-level planning model

This section presents the mathematical formulation of the proposed scenario-based stochastic planning model of IEGS. It is formulated according to the wind power-related scenarios presented in Section 2. Although the scenario generation method is better able to describe the uncertainty of energy demand, it may not reflect the seasonal character of energy demand. Thus, two typical load curves are adopted for the modeling of energy load, representing: (a) a high-electrical load/low-gas load situation; and (b) a high-gas load/low-electrical load situation. These two situations reflect the typical energy demands for summer and winter, respectively, in China. In the proposed model, the investment costs are analyzed on an annual basis. The operational costs are therefore annualized to make them comparable to the investment costs. A time-series operational model is used to capture the time-correlated relationships of gas storage and wind power [14].

3.1. Objective function

The proposed planning model aims to minimize the total present value of the investment costs and operational costs of an IEGS within the planning horizon (see Eq. (10)). Eq. (11) relates to the investment costs of gas/coal-fired generators, wind farms, new transmission lines, PtG facilities, natural gas storage units and new gas pipelines.$\kappa = 1/(1+r)^{h-1}$ is the present-worth coefficient, in which r is a discount rate and h is the planning year. Eq. (12) represents the IEGS operational costs for BS, SVS and ERS within the planning horizon. The operational costs are composed of: the fuel costs of candidate and existing coal-fired generators; the gas production fee; the operational cost of gas storage; and the carbon emission fee for generators. Note that the fuel cost of gas-fired generators is considered in terms of the gas production fee. Note, also, that the minimization of the operational costs of gas storage in Eq (12) prevents gas from being stored and released at the same time.

$$\min(IC + OC) \tag{10}$$

$$IC = \sum_h \kappa \begin{pmatrix} \sum_{i \in CG} C_i^{inv}(y_i^h - y_i^{h-1}) + \sum_{j \in CW} C_j^{inv}\left(y_j^h - y_j^{h-1}\right) \\ + \sum_{l \in CL} C_l^{inv}(y_l^h - y_l^{h-1}) + \sum_{a \in CA} C_a^{inv}(z_a^h - z_a^{h-1}) \\ + \sum_{k \in CS} C_k^{inv}(z_k^h - z_k^{h-1}) + \sum_{p \in CP} C_p^{inv}(z_p^h - z_p^{h-1}) \end{pmatrix} \tag{11}$$

$$OC = \sum_h \kappa \sum_b \rho_b^L \sum_\omega \rho_\omega^W \sum_{t \in T} \begin{bmatrix} \sum_{i \notin GU} C_i^{fuel} P_{i,t,b}^{\omega,h} + \sum_{s \in GS} C_s^{gas} F_{s,t,b}^{\omega,h} \\ + \sum_{k \in CS} C_k^{ope}(Q_{k,t,b}^{\omega,h} + D_{k,t,b}^{\omega,h}) \\ + \sum_{i \in CG \cup EG} C_i^{EM} P_{i,t,b}^{\omega,h} \end{bmatrix} \tag{12}$$

3.2. Investment constraints

The planning constraints consist of commissioning time constraints (13)–(18) and generation capacity adequacy constraints (19). Once a candidate element is installed, its investment state is changed to 1 for the remaining years (13)–(18). Constraint (19) ensures that the total generation capacity of the existing generators and installed candidate generators can meet the forecasted electrical load plus system reserve.

$$y_i^{h-1} \leqslant y_i^h, \quad i \in CG \tag{13}$$

$$y_j^{h-1} \leqslant y_j^h, \quad j \in CW \tag{14}$$

$$y_l^{h-1} \leqslant y_l^h, \quad l \in CL \tag{15}$$

$$z_a^{h-1} \leqslant z_a^h, \quad a \in CA \tag{16}$$

$$z_k^{h-1} \leqslant z_k^h, \quad a \in CS \tag{17}$$

$$z_p^{h-1} \leqslant z_p^h, \quad a \in CP \tag{18}$$

$$\sum_{i \in CG} y_i^h P_i^{\max} + \sum_{i \in EG} P_i^{\max} \geqslant \sum_{e \in PL} P_{e,t,b}^h (1 + R_b^h) \tag{19}$$

3.3. Operational constraints

The constraints (20)–(31) pertain to power system operation while (32)–(46) pertain to natural gas system operation. Eqs. (47)–(48) describe the coupled relationship of the two systems. Eqs. (20)–(23) reflect the capacity limits of existing and candidate generators, PtG facilities and wind farms. Eqs. (24)–(25) refer to the ramping rates of generators and PtG facilities. DC power flow model is adopted to model the existing and candidate transmission lines by (26)-(29). The limits on the bus phase angles are shown in constraint (30). Eq. (31) represents the power balance of the power system bus. Limits on the production of gas wells and the nodal gas pressure are shown in Eqs. (32)–(33). Eqs. (34)–(36) capture the gas flow limits of the compressor, the relationship between the inlet and outlet pressures of the compressor and the gas consumed by the compressor, respectively. Generally, the gas consumed by the compressor is 3–5% of the gas it transports [37].The existing and candidate pipeline gas flows can be modeled using the Weymouth equation as (37)–(40). Eqs. (41)–(43) respectively limit injection/withdraw rates of gas storage and the capacity of gas storage. The gas stored in the gas storage at the final hour should be the same as the initial gas stored as (44). Eq. (45) denotes the relationship between the gas stored in gas storage over two continuous periods. Eq. (46) describes the nodal gas balance. Electricity and gas systems can be linked by gas-fired generators and PtG faciliteis. To formulate the MILP planning model, the energy conversion relationships are linearized. The

gas consumed by gas-fired generators is thus linearized as (47). In contrast, the gas produced by PtG is proportional to the power consumed in (48). Note that the pipeline linepack is usually balanced by taking the initial value at the end of the operational dispatch. For long dispatch interval in the planning model, the pipeline linepack has little effect on the gas flow. Hence, the pipeline linepack is generally considered in the operational model rather than planning model.

$$0 \leqslant P_{i,t,b}^{\omega,h} \leqslant P_i^{\max}, \quad i \in EG \tag{20}$$

$$0 \leqslant P_{i,t,b}^{\omega,h} \leqslant P_i^{\max} y_i^h, \quad i \in CG \tag{21}$$

$$0 \leqslant P_{a,t,b}^{\omega,h} \leqslant P_a^{\max} z_a^h, \quad a \in CA \tag{22}$$

$$0 \leqslant P_{j,t,b}^{\omega,h} \leqslant P_{j,t}^{\omega,\max} y_j^h, \quad j \in CW \tag{23}$$

$$-P_i^{RD} \leqslant P_{i,t,b}^{\omega,h} - P_{i,t-1,b}^{\omega,h} \leqslant P_i^{RU}, \quad i \in EG \cup CG \tag{24}$$

$$P_a^{RD} \leqslant P_{a,t,b}^{\omega,h} - P_{a,t-1,b}^{\omega,h} \leqslant P_a^{RU}, \quad a \in CA \tag{25}$$

$$P_{l,t,b}^{\omega,h} = B_{l(mn)}(\theta_{m(l),t,b}^{\omega,h} - \theta_{n(l),t,b}^{\omega,h}), \; l \in EL \tag{26}$$

$$-P_l^{\max} \leqslant P_{l,t,b}^{\omega,h} \leqslant P_l^{\max}, \; l \in EL \tag{27}$$

$$|P_{l,t,b}^{\omega,h} - B_{l(mn)}(\theta_{m(l),t,b}^{\omega,h} - \theta_{n(l),t,b}^{\omega,h})| \leqslant M(1 - y_l^h), \; l \in CL \tag{28}$$

$$|P_{l,t,b}^{\omega,h}| \leqslant P_l^{\max} y_l^h, \; l \in CL \tag{29}$$

$$-\theta_m^{\max} \leqslant \theta_{m,t,b}^{\omega,h} \leqslant \theta_m^{\max}, \; m \in PB \tag{30}$$

$$\sum_{i \in E(m)} P_{i,t,b}^{\omega,h} + \sum_{j \in E(m)} P_{j,t,b}^{\omega,h} - \sum_{a \in E(m)} P_{a,t,b}^{\omega,h} - \sum_{l \in E(m)} P_{l,t,b}^{\omega,h} = \sum_{e \in E(m)} P_{e,t,b}^{h} \tag{31}$$

$$0 \leqslant F_{s,t,b}^{\omega,h} \leqslant F_s^{\max}, \quad s \in GS \tag{32}$$

$$\pi_n^{\min} \leqslant \pi_{n,t,b}^{\omega,h} \leqslant \pi_n^{\max}, \quad n \in GN \tag{33}$$

$$F_c^{\min} \leqslant F_{c,t,b}^{\omega,h} \leqslant F_c^{\max}, \quad c \in GC \tag{34}$$

$$R_c^{\min} \pi_{m(c),t,b}^{\omega,h} \leqslant \pi_{n(c),t,b}^{\omega,h} \leqslant R_c^{\max} \pi_{m(c),t,b}^{\omega,h}, \quad c \in GC \tag{35}$$

$$\tau_{c,t,b}^{\omega,h} = 0.03 * F_{c,t,b}^{\omega,h}, \quad c \in GC \tag{36}$$

$$F_{p,t,b}^{\omega,h} \, |F_{p,t,b}^{\omega,h}| = C_{mn}^2(\pi_{m(p),t,b}^{2,\omega,h} - \pi_{n(p),t,b}^{2,\omega,h}), \quad p \in EP \tag{37}$$

$$-F_p^{\max} \leqslant F_{p,t,b}^{\omega,h} \leqslant F_p^{\max}, \; p \in EP \tag{38}$$

$$|F_{p,t,b}^{\omega,h} \, |F_{p,t,b}^{\omega,h}| - C_{mn}^2(\pi_{m(p),t,b}^{2,\omega,h} - \pi_{n(p),t,b}^{2,\omega,h})| \leqslant M(1 - z_p^h), \; p \in CP \tag{39}$$

$$|F_{p,t,b}^{\omega,h}| \leqslant F_p^{\max} z_p^h, \; p \in CP \tag{40}$$

$$0 \leqslant Q_{k,t,b}^{\omega,h} \leqslant Q_k^{\max} z_k^h, \; k \in CS \tag{41}$$

$$0 \leqslant D_{k,t,b}^{\omega,h} \leqslant D_k^{\max} z_k^h, \; k \in CS \tag{42}$$

$$S_k^{\min} z_k^h \leqslant S_{k,t,b}^{\omega,h} \leqslant S_k^{\max} z_k^h, \; k \in CS \tag{43}$$

$$S_{k,NT,b}^{\omega,h} = z_k^h S_{k,0}, \; k \in CS \tag{44}$$

$$S_{k,t,b}^{\omega,h} = S_{k,t-1,b}^{\omega,h} + \eta_k^c Q_{k,t,b}^{\omega,h} - D_{k,t,b}^{\omega,h}/\eta_k^d, \; k \in CS \tag{45}$$

$$\begin{aligned} &\sum_{s \in G(n)} F_{s,t,b}^{\omega,h} + \sum_{k \in G(n)} Q_{k,t,b}^{\omega,h} - \sum_{k \in G(n)} D_{k,t,b}^{\omega,h} \\ &+ \sum_{a \in G(n)} F_{a,t,b}^{\omega,h} - \sum_{i \in G(n)} F_{i,t,b}^{\omega,h} - \sum_{p \in G(n)} F_{p,t,b}^{\omega,h} \\ &- \sum_{c \in G(n)} F_{c,t,b}^{\omega,h} - \sum_{c \in G(n)} \tau_{c,t,b}^{\omega,h} = \sum_{d \in G(n)} F_{d,t,b}^{h} \end{aligned} \tag{46}$$

$$F_{i,t,b}^{\omega,h} = \beta_i P_{i,t,b}^{\omega,h}/GHV, \; i \in GU \tag{47}$$

$$F_{a,t,b}^{\omega,h} = \chi \alpha_a P_{a,t,b}^{\omega,h}/GHV, \; a \in CA \tag{48}$$

4. Solution methodology

Although the wind power scenarios are limited, the proposed planning model is still a large-scale MINLP optimization problem when considering both the wind power scenarios and load curves. The planning model was therefore first reformulated into a MILP problem by linearizing the Weymouth equations. Then, a bi-level iterative process based on Benders Decomposition was used to provide an efficient solution to the planning problem. The planning problem was separated into an upper-level planning problem and lower-level feasibility and optimality check problem. The upper-level planning problem is to determine the candidate IEGS assets associated with the investment constraints, the BS-based operational constraints and Benders cuts. In the lower-level, the planning solution is checked against the SVS and ERS-related operational problems to generate a feasibility cut or optimality cut for the upper-level problem.

4.1. MILP problem reformulation

As it stands, the planning model is intractable because of the nonlinear and nonconvex gas flow constraints (37), (39). Thus, incremental piecewise linearization method was adopted to convert the problem into a MILP problem [17]. Introducing $\Pi_{n,t}^{\omega,h} = \pi_{n,t}^{2,\omega,h}$ into Eq. (37), it can be reformulated as follows:

$$F_{p,t,b}^{\omega,h} = F_p^{(1)} + \sum_{r=1}^{N_p} (F_p^{(r+1)} - F_p^{(r)}) \delta_{p,t,b}^{r,\omega,h}, \; p \in EP \tag{49}$$

$$\begin{aligned} &F_p^{(1)} \, |F_p^{(1)}| + \sum_{r=1}^{N_p} (F_p^{(r+1)} \, |F_p^{(r+1)}| - F_p^{(r)} \, |F_p^{(r)}|) \delta_{p,t,b}^{r,\omega,h} \\ &\quad = C_{mn}^2(\Pi_{m(p),t,b}^{\omega,h} - \Pi_{n(p),t,b}^{\omega,h}) \end{aligned} \tag{50}$$

$$\begin{aligned} &0 \leqslant \delta_{p,t,b}^{r,\omega,h} \leqslant 1, \;\; \delta_{p,t,b}^{r+1,\omega,h} \leqslant \varsigma_{p,t,b}^{r,\omega,h} \leqslant \delta_{p,t,b}^{r,\omega,h}, \\ &\quad \varsigma_{p,t,b}^{r,\omega,h} \in \{0, 1\}, \; r = 1, \cdots, N_p - 1 \end{aligned} \tag{51}$$

Similarly, (39) is converted into following linear constraints:

$$\begin{aligned} &|F_{p,t,b}^{\omega,h} - F_p^{(1)} - \textstyle\sum_{r=1}^{N_p} (F_p^{(r+1)} - F_p^{(r)}) \delta_{p,t,b}^{r,\omega,h}| \\ &\leqslant M(1 - z_p^h), \; p \in CP \end{aligned} \tag{52}$$

$$\begin{aligned} &\left| \begin{array}{l} \sum_{r=1}^{N_p} (F_p^{(r+1)} \, |F_p^{(r+1)}| - F_p^{(r)} \, |F_p^{(r)}|) \delta_{p,t,b}^{r,\omega,h} + \\ F_p^{(1)} \, |F_p^{(1)}| - C_{mn}^2(\Pi_{m(p),t,b}^{\omega,h} - \Pi_{n(p),t,b}^{\omega,h}) \end{array} \right| \\ &\leqslant M(1 - z_p^h), \; p \in CP \end{aligned} \tag{53}$$

Once turned into a MILP problem, the proposed model can be stated in a compact form:

$$\min \;\; A^T x + \sum_{\omega=1} B^T y^\omega \tag{54-a}$$

$$s.t \quad Cx \leqslant 0 \tag{54-b}$$

$$Dx + Ey^\omega \leqslant a^\omega \tag{54-c}$$

$$Ky \leqslant c^\omega \tag{54-d}$$

where x represents the investment binary variables of the candidate assets determined at the upper level, and y represents the continuous operational variables for the different scenarios. $A^T x$ indicates the investment cost in Eq. (11) and $B^T y^\omega$ represents the operation costs for each scenario in Eq. (12). The constraints encapsulated in Eq. (54-b) correspond to investment constraints (13)–(19). The set of constraints

in Eq. (54-c) consist of the capacity constraints for the candidate generators, PtG and wind farms (20)–(23), the power transmission constraints for the candidate transmission line (28)–(29), the gas flow constraints for the alternative pipelines (39)–(40), and the operational constraints for the candidate gas storage (41)–(44). The set of constraints (54-d) relate to the other constraints of operational constraints.

4.2. Upper-Level planning problem

The upper-level planning problem is to minimize the investment cost and operational cost of the BS with respect to the planning constraints, BS-based operational constraints, Benders feasibility cuts and optimality cuts. The upper-level planning problem determines the approximate candidates for gas/coal-fired generators, wind farms, transmission lines, PtG facilities, gas storage units and pipelines. The upper-level planning problem can be described as follows:

$$\min \quad Z$$

$$Z \geqslant A^T x + B^T y^{\omega} + OC_o^{Sum} + CU_o^O, \quad \omega = 1\,(BS) \tag{55-a}$$

$$s.t \quad Cx \leqslant 0 \tag{55-b}$$

$$Dx + Ey^{\omega} \leqslant a^{\omega} \tag{55-c}$$

$$Ky^{\omega} \leqslant c^{\omega} \tag{55-d}$$

$$CU^F \leqslant 0 \tag{55-e}$$

The third and fourth terms of the objective function in (55-a) are respectively the accumulated operation cost and the optimality cut for the lower-level problems of rank o. The constraints (55-e) correspond to the Benders feasibility cuts. The accumulated operation cost, optimality cut and feasibility cuts are covered by the description of the lower-level problem.

4.3. Lower-level feasibility and optimality problem

Once the alternative candidates have been identified by the upper-level planning problem, the feasibility of the determined assets can be assessed through SVS and ERS-based operational problems. The lower-level problem relating to scenario ω can be described in the following way:

$$\min \ B^T y^{\omega}, \quad (\omega > 1, \ SVS, \ ERS) \tag{56-a}$$

$$s.t \quad D\widehat{x} + Ey^{\omega} \leqslant a^{\omega} \tag{56-b}$$

$$Ky \leqslant c^{\omega} \tag{56-c}$$

The objective in (56-a) is to minimize the IEGS operation cost for scenario ω. The binary variable $\widehat{x}$ in the operational constraints (56-b) are fixed as values obtained from the upper-level planning solution. If the lower-level check problem of scenario ω is infeasible, the corresponding feasibility cut shown in (57) can be generated and added to the feasibility cuts in the upper-level planning problem as the constraints (55-e).

$$\begin{aligned}
CU_q^F = & \sum_{i\in CG} \lambda_{i,t,b}^{\omega,h} P_i^{\max}(y_i^h - \widehat{y}_i^h) + \sum_{a\in CA} \mu_{a,t,b}^{\omega,h} P_a^{\max}(z_a^h - \widehat{z}_a^h) \\
& + \sum_{j\in CW} \phi_{j,t,b}^{\omega,h} P_{j,t,\omega}^{\omega,max}(y_j^h - \widehat{y}_j^h) \\
& + \sum \begin{bmatrix} (\bar{\psi}_{l,t,b}^{\omega,h} + \underset{-}{\psi}_{l,t,b}^{\omega,h}) P_l^{\max}(y_l^h - \widehat{y}_l^h) \\ -(\bar{\varphi}_{l,t,b}^{\omega,h} + \underset{-}{\varphi}_{l,t,b}^{\omega,h}) M(y_l^h - \widehat{y}_l^h) \end{bmatrix} \\
& + \sum_{k\in CS} \begin{bmatrix} \sigma_{k,t,b}^{D,\omega,h} D_k^{max}(z_k^h - \widehat{z}_k^h) + \sigma_{k,t,b}^{Q,\omega,h} Q_k^{max}(z_k^h - \widehat{z}_k^h) \\ +\bar{\sigma}_{k,t,b}^{S,\omega,h} S_k^{max}(z_k^h - \widehat{z}_k^h) - \underset{-}{\sigma}_{k,t,b}^{Q,\omega,h} S_k^{min}(z_k^h - \widehat{z}_k^h) \end{bmatrix} \\
& + \sum_{l\in CP} \begin{bmatrix} (\bar{\tau}_{p,t,b}^{\omega,h} + \underset{-}{\tau}_{p,t,b}^{\omega,h}) F_p^{max}(z_p^h - \widehat{z}_p^h) \\ -(\bar{\upsilon}_{p,t,b}^{\omega,h} + \underset{-}{\upsilon}_{p,t,b}^{\omega,h}) M(z_p^h - \widehat{z}_p^h) \\ -(\bar{\xi}_{p,t,b}^{\omega,h} + \underset{-}{\xi}_{p,t,b}^{\omega,h}) M(z_p^h - \widehat{z}_p^h) \end{bmatrix} \leqslant 0
\end{aligned} \tag{57}$$

$$\begin{aligned}
CU_o^O = & CU_o^O + \sum_{i\in CG} \lambda_{i,t,b}^{\omega,h} P_i^{\max}(y_i^h - \widehat{y}_i^h) \\
& + \sum_{a\in CA} \mu_{a,t,b}^{\omega,h} P_a^{max}(z_a^h - \widehat{z}_a^h) + \sum_{j\in CW} \phi_{j,t,b}^{\omega,h} P_{j,t,\omega}^{\omega,max}(y_j^h - \widehat{y}_j^h) \\
& + \sum_{l\in CL} \begin{bmatrix} (\bar{\psi}_{l,t,b}^{\omega,h} + \underset{-}{\psi}_{l,t,b}^{\omega,h}) P_l^{max}(y_l^h - \widehat{y}_l^h) \\ -(\bar{\varphi}_{l,t,b}^{\omega,h} + \underset{-}{\varphi}_{l,t,b}^{\omega,h}) M(y_l^h - \widehat{y}_l^h) \end{bmatrix} \\
& + \sum_{k\in CS} \begin{bmatrix} \sigma_{k,t,b}^{D,\omega,h} D_k^{max}(z_k^h - \widehat{z}_k^h) + \sigma_{k,t,b}^{Q,\omega,h} Q_k^{max}(z_k^h - \widehat{z}_k^h) \\ +\bar{\sigma}_{k,t,b}^{S,\omega,h} S_k^{max}(z_k^h - \widehat{z}_k^h) - \underset{-}{\sigma}_{k,t,b}^{Q,\omega,h} S_k^{min}(z_k^h - \widehat{z}_k^h) \end{bmatrix} \\
& + \sum_{l\in CP} \begin{bmatrix} (\bar{\tau}_{p,t,b}^{\omega,h} + \underset{-}{\tau}_{p,t,b}^{\omega,h}) F_p^{max}(z_p^h - \widehat{z}_p^h) \\ -(\bar{\upsilon}_{p,t,b}^{\omega,h} + \underset{-}{\upsilon}_{p,t,b}^{\omega,h}) M(z_p^h - \widehat{z}_p^h) \\ -(\bar{\xi}_{p,t,b}^{\omega,h} + \underset{-}{\xi}_{p,t,b}^{\omega,h}) M(z_p^h - \widehat{z}_p^h) \end{bmatrix}
\end{aligned} \tag{58}$$

where $\lambda_{i,t,b}^{\omega,h}$, $\mu_{a,t,b}^{\omega,h}$, $\phi_{j,t,b}^{\omega,h}$, $\varphi_{l,t,b}^{\omega,h}$, $\psi_{l,t,b}^{\omega,h}$, $\xi_{p,t,b}^{\omega,h}$, $\gamma_{p,t,b}^{\omega,h}$, $\upsilon_{p,t,b}^{\omega,h}$ and $\sigma_{k,t,b}^{\omega,h}$ are dual values of the constraints associated with the candidate generators, PtG facilities, wind farms, transmission lines, gas storage units and pipelines.

When the lower-level operational check problem of scenario ω is feasible, the optimality cut and the operation cost and are accumulated as per Eqs. (58)–(59).

$$OC_o^{Sum} = OC_o^{Sum} + B^T y^{\omega} \tag{59}$$

4.4. Summary

As both the upper-level and lower-level problems are MILP problems, they can be iteratively solved by commercial solvers such as Cplex or Gurobi until an optimal IEGS planning solution is obtained. Fig. 1 depicts the flowchart of proposed bi-level planning model, including the following detailed steps:

Step 1: Initialize the lower bound (LB), upper bound (UB), initial operating cost, $OC_0^{Sum} = 0$ and initial optimality cut $CU_0^O = 0$. Set the tolerance $\varepsilon = 0.9999$, $q = 0$, $o = 0$.

Step 2: Solve the upper-level planning problem and update the LB as the value of upper-level problem objective. Set $\omega = 1$.

Step 3: Set $\omega = \omega + 1$ and solve the lower-level feasibility and optimality problems of scenario ω by fixing the binary variables as values obtained from Step 2. If the lower-level problem is infeasible, feed the feasibility cut to the upper-level problem. Set $q = q + 1$ and return to step 2. If the lower-level problem is feasible, accumulate the optimality

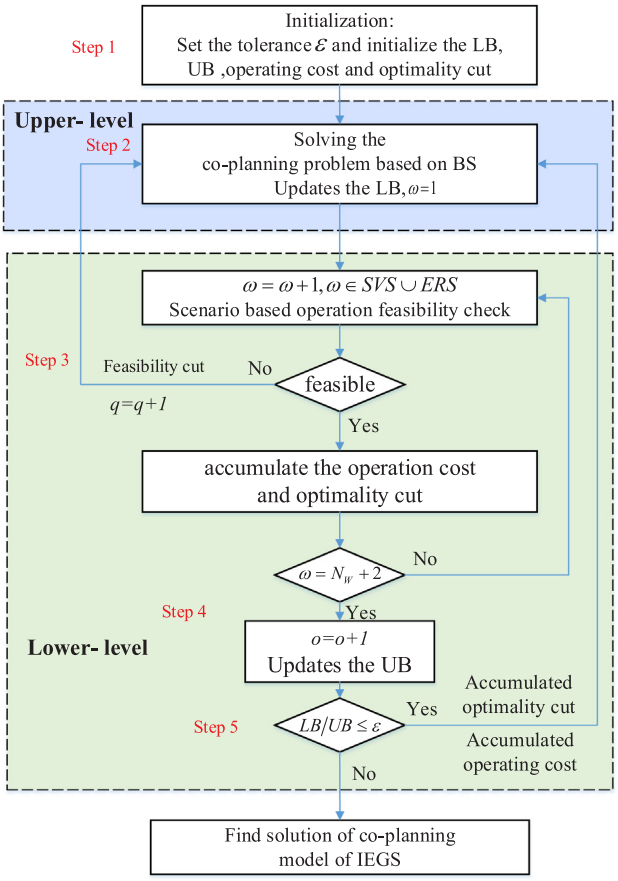

Fig. 1. Flowchart of proposed bi-level planning model of IEGS.

cut and operation cost as Eqs. (58)-(59).

Step 4: As presented in Section II, there are total of $N_W + 3$ wind power scenarios, including one BS, $N_W = 2^K$ SVS, and two ERS. If $\omega < N_W + 3$, the process will go back to step 3. Otherwise, set $o = o + 1$ and update the UB as (60).

$$UB = IC + B^T y^{\omega=1} + OC_o^{Sum} \tag{60}$$

where IC and $B^T y^{\omega=1}$ are values obtained from Step 2.

Step 5: Check the stop criteria: If $LB/UB \leqslant \varepsilon$, add the accumulated operation cost and accumulated optimality cut to the upper-level planning problem and go to step 2. Otherwise, the optimal IEGS planning solution has been converged to, stop.

5. Case studies

In this section, a modified IEEE 39-bus power system and a Belgium 20-node gas system are first used to demonstrate the effectiveness of the proposed bi-level planning model through numerical comparisons. Then, a second test case is examined using a modified real provincial power system with natural gas system in northwestern China. This is to show the application of the planning model in practice. The carbon emission fee is 6$/MWh and the mean fuel cost of the coal-fired generators is 24.2$/MWh. The mean gas production fee is 46$ kcf. The big-M parameter M is set at 1e+06. The discount rate is 5% and the optimality gap is set at 0.01%. 13 segments are adopted in the piecewise linearization of the Weymouth equation as a tradeoff between computational efficiency and solution accuracy. The numerical tests were performed using Matlab 2014a and Gurobi 6.5.0 on a PC with an Inter (R) Core(TM) i7-4790 CPU(3.6 GHz) and 16 GB of memory.

5.1. Modified IEEE 39-bus-20-gas-node IEGS

The modified 39-bus-20-gas-node IEGS is composed of 6 coal-fired generators, 44 lines, 21 electrical loads, 2 gas sources, 17 pipelines, 2 compressor stations and 10 non-power gas loads. The candidate components consist of 4 coal-fired generators, 4 gas-fired generators, 3 wind farms, 16 transmission lines, 3 PtG facilities, 4 natural gas storage units and 7 pipelines. The topology is shown in Fig. 2 and the candidate components are colored red and ranked. Other detailed parameters of the small-scale test system are available in [38]. The test assumes a 5-

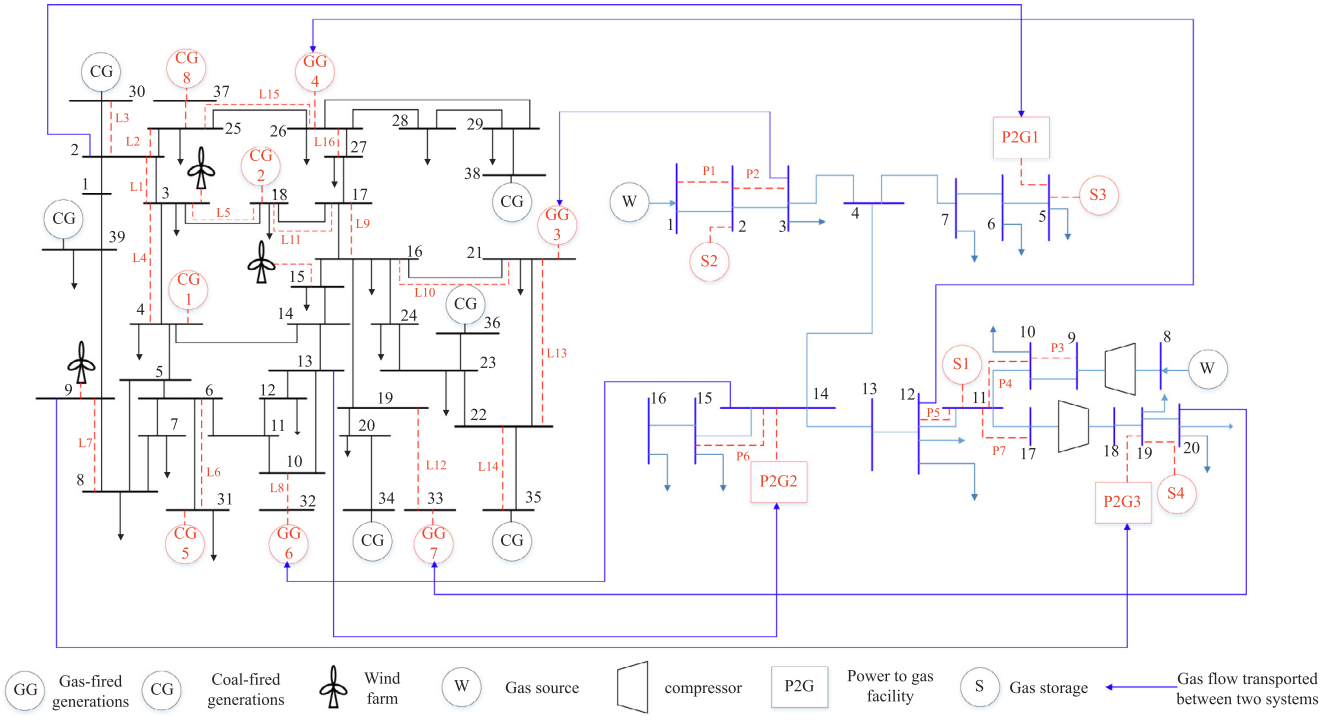

Fig. 2. Topology of the modified IEEE 39-bus-20-gas-node test IEGS.

year planning horizon with two 24-h load curves. The base electrical load and non-power gas load in the first planning year are, respectively, 6254.2 MW and 2739.62kcf/h, with average growth rates of 4% and 5%. As natural gas is a scarce resource in China, the load scenarios in the tests assume a situation where gas is scarce to assess the role of PtG and gas storage in mitigating the shortage in gas supply. The profiles of the electrical and gas loads in the form of two 24-h load curves are shown in Fig. 3. Load curve 1 represents a high electric load and a low gas load, while load curve 2 is the opposite. These two load curves represent summer and winter IEGS load scenarios, respectively.

Five cases are considered to illustrate the proposed scenario-based planning model of IEGS:

Case 1: co-optimization planning of IEGS by the proposed scenario-based bi-level decomposition algorithm.
Case 2: No gas storage-As case 1, but with no candidate gas storage units in the IEGS.
Case 3: No wind power uncertainty-As case 1, but with only the BS of wind power being considered in the planning model.
Case 4: No Weymouth equation-As case 1, but with only the linear transportation gas flow model expressed by Eqs. (38) and, being taken into account.
Case 5: No PtG-As case 1, but with no candidate PtG facilities in the IEGS.

(1) Planning Results for Two Load Curves

The planning results for case 1–5 using the two load curves are shown in Table 1, with the two subscripts representing the indices and installation year of the candidate assets. The total cost of the planning investments and operation cost in Table 1 are summarized in Table 2.

Case 1: At the end of the planning horizon, all eight of the candidate thermal generators and three wind farms have been installed to meet the forecast electric load. PtG A1 and A2 have been installed to convert excess renewable energy into natural gas. Seven transmission lines and five gas pipelines have been constructed to deliver energy. Meanwhile, three gas storage units have been installed to balance the energy needs at different periods and to mitigate gas supply shortage.

Case 2: Load curve 1 is infeasible for case 2 because there is no candidate gas storage to make up for gas demand shortages during peak gas load hours.

Case 3: When compared to case 1, the wind farm W3 is uninstalled. Thus, the BS is not able to represent the wind power stochasticity. Since the available wind power in some SVSs and ERSs is higher than the available wind power in the BS, the operation of the wind farms in SVS and ERS is more profitable than operation of the wind farms in BS. There were more wind farms installed in case 1. As there are fewer here, the fluctuation of wind power in the BS is smaller, which means a smaller generator capacity is needed to balance power fluctuation. Consequently, in comparison to case 1, generator G4 with a smaller capacity is installed earlier while generator G7 is installed later. Meanwhile, transmission lines L9 and L12 are built for power delivery in the same years as G4 and G7, respectively. In addition, the minimum wind power in the BS is not as low as the minimum wind power in the SVS and ERS. This means the energy shortage in the BS is less than it is in the SVS and ERS in some specific situations. Gas storage S1 is therefore not installed to make up for energy shortages. Neither are pipelines P1 and P2 installed to ensure gas delivery under specific situations. Thus, it can be seen that the modelling of the wind power has a great effect on the planning results. The combination of the BS, SVS and ERS are representative of the uncertainty of wind power.

Case 4: Unlike case 1, here, pipelines P1 and P2 are not constructed. The maximum gas flow transportation ability of the pipelines in case 4 is larger than it is in case 1 because there is no limitation arising from the pressure drop along the pipelines. With a larger gas transportation ability, the existing pipelines of P1 and P2 are sufficient for gas delivery. Thus, there is no need to expand to a new P1 and P2. In addition, pipeline P3 is installed later than it is in case 1 because the existing pipelines have a larger gas transportation ability.

Case 5: Without a candidate PtG to supplement the gas supply, case 5 is infeasible for both load curves due to the lack of natural gas. Thus, PtG also plays an important role in supplementing the natural gas supply.

(2) Planning Results for One Load Curve

The planning model was also applied to just load curve 2 to analyze the relationship between investment prioritization and load levels. Table 3 illustrates the planning results for cases 1–5 just considering load curve 2. The total costs of the available cases in Table 3 are summarized in Table 4. The total costs of cases 1–4 in Table 4 are all lower than the corresponding total costs in Table 2. This is because the average energy need for two load curves is higher than it is for just load curve 2. As the electric load of load curve 2 is lower than electric load of load curve 1, fewer generators and transmission lines need to be installed. Though the non-power gas load of load curve 2 is higher than that of load curve 1, fewer gas storage units and pipelines need to be installed. This indicates that the gas consumed to generate electricity accounts for a large proportion of the total gas load.

Case 1: As the electric load of load curve 2 is low, only 2 gas-fired generators and 3 coal-fired generators are installed. The installation of the coal-fired generators comes first because of the lower fuel cost.

Case 2: Without a candidate gas storage unit to make up for gaps in the gas supply, the gas consumed to generate power has to be reduced to ensure the gas supply for the non-power gas load. When compared to case 1, the gas-fired generator G3 is installed instead of G7, which leads to 252 MW reduction of the gas-fired generator capacity. Wind farm W3 is not installed due to the lack of fast responding generator capacity to accommodate wind power. Meanwhile, transmission lines L9, L11, and L14 have to be constructed to transmit the coal-fired generator power. More wind spillage results in the operation cost increasing from 1.4222B$ to 1.4334B$. So, the gas storage affects the planning results because it allows for meeting the gas demand at peak hours. It also influences the installation of transmission lines.

Case 3: When wind uncertainty is not considered, the total cost is reduced to 2.5856B$. This is because the total installed generator capacity, wind power capacity and storage capacity are reduced. Unlike in case 1, wind farm W3 is not installed due to its inadequate operational profit in the BS. A smaller generator capacity is required to accommodate the wind power because the wind power fluctuations smaller. As the minimum wind power of the BS is higher, the energy shortage at peak hours is not that severe. Thus, gas storage S1 is not installed.

Case 4: The planning results in case 4 are the same as in case 1. Though the gas load of curve 2 is higher, the total gas demand is lower on account of there being less gas consumed to generate electricity.

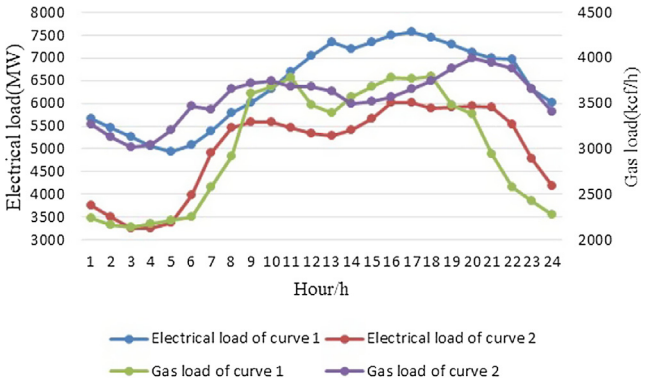

Fig. 3. Profiles of the electric and gas 24-h loads.

Table 1
Comparison of Cases 1–4 with Two Load Curves.

Case	Constructed components
1	$G_{1,1}$,$G_{2,1}$,$G_{3,1}$,$G_{4,4}$,$G_{5,1}$,$G_{6,2}$,$G_{7,1}$,$G_{8,1}$,$W_{1,1}$,$W_{2,1}$,$W_{3,1}$,$A_{1,1}$,$A_{2,1}$, $S_{1,3}$,$S_{3,5}$,$S_{4,3}$,$L_{1,1}$,$L_{3,1}$,$L_{4,1}$,$L_{8,2}$,$L_{11,1}$,$L_{12,1}$,$L_{14,1}$,$P_{1,5}$,$P_{2,5}$,$P_{3,2}$,$P_{4,4}$,$P_{6,1}$
2	Infeasible
3	$G_{1,1}$,$G_{2,1}$,$G_{3,1}$,$G_{4,1}$,$G_{5,1}$,$G_{6,2}$,$G_{7,4}$,$G_{8,1}$,$W_{1,1}$,$W_{2,1}$, $A_{1,1}$,$A_{2,1}$,$S_{3,5}$,$S_{4,2}$,$L_{1,1}$,$L_{3,1}$,$L_{4,1}$,$L_{8,2}$,$L_{9,1}$,$L_{11,1}$,$L_{12,4}$,$L_{14,1}$,$P_{3,3}$,$P_{4,4}$,$P_{6,1}$
4	$G_{1,1}$,$G_{2,1}$,$G_{3,1}$,$G_{4,4}$,$G_{5,1}$,$G_{6,2}$,$G_{7,1}$,$G_{8,1}$,$W_{1,1}$,$W_{2,1}$,$W_{3,1}$, $A_{1,1}$,$A_{2,1}$,$S_{1,5}$,$S_{3,5}$,$S_{4,2}$,$L_{1,1}$,$L_{3,1}$,$L_{4,1}$,$L_{8,2}$,$L_{11,1}$,$L_{12,1}$,$L_{14,1}$,$P_{3,3}$,$P_{4,4}$,$P_{6,1}$
5	Infeasible

Table 2
Comparison of planning costs with Two Load Curves.

Cost(B$)		1	2	3	4	5
Investment cost	Generator unit	0.6666	–	0.6657	0.6666	–
	Wind farm	0.5040	–	0.4140	0.5040	–
	PtG	0.2400	–	0.2400	0.2400	–
	Gas storage	0.0354	–	0.0291	0.0351	–
	Transmission lines	0.0882	–	0.0937	0.0882	–
	Pipelines	0.0941	–	0.0796	0.0795	–
Operation cost		1.4655	–	1.4589	1.4654	–
Total cost		3.0940	–	2.9811	3.0789	–

Table 3
Comparison of Cases 1–5 with Load Curve 2.

Case	Constructed components
1	$G_{1,1}$,$G_{2,1}$,$G_{4,2}$,$G_{5,1}$,$G_{7,4}$,$W_{1,1}$,$W_{2,1}$,$W_{3,1}$, $A_{1,1}$,$A_{2,1}$,$S_{1,5}$,$S_{4,5}$,$L_{1,3}$,$L_{3,2}$,$L_{4,1}$,$L_{12,4}$,$P_{3,4}$,$P_{6,1}$
2	$G_{1,1}$,$G_{2,1}$,$G_{3,2}$,$G_{4,4}$,$G_{5,1}$,$W_{1,1}$,$W_{2,1}$, $A_{1,1}$,$A_{2,1}$,$L_{1,1}$,$L_{3,1}$,$L_{4,1}$,$L_{9,2}$,$L_{11,2}$,$L_{14,4}$,$P_{3,4}$,$P_{6,1}$
3	$G_{1,1}$,$G_{2,1}$,$G_{3,2}$,$G_{4,4}$,$G_{5,1}$,$W_{1,1}$,$W_{2,1}$, $A_{1,1}$,$A_{2,1}$,$S_{4,5}$,$L_{1,1}$,$L_{3,1}$,$L_{4,1}$,$L_{9,2}$,$L_{11,2}$,$P_{3,4}$,$P_{6,1}$
4	$G_{1,1}$,$G_{2,1}$,$G_{4,2}$,$G_{5,1}$,$G_{7,4}$,$W_{1,1}$,$W_{2,1}$,$W_{3,1}$, $A_{1,1}$,$A_{2,1}$,$S_{1,5}$,$S_{4,5}$,$L_{1,3}$,$L_{3,2}$,$L_{4,1}$,$L_{12,4}$,$P_{3,4}$,$P_{6,1}$
5	Infeasible

Table 4
Comparison of planning costs with Load Curve 2.

Cost(B$)		Case 1	Case 2	Case 3	Case 4
Investment cost	Generator unit	0.4232	0.3937	0.3937	0.4232
	Wind farm	0.5040	0.4140	0.4140	0.5040
	PtG	0.2400	0.2400	0.2400	0.2400
	Gas storage	0.0106	–	0.0047	0.0106
	Transmission lines	0.0516	0.0665	0.0566	0.0516
	Pipelines	0.0436	0.0436	0.0436	0.0436
Operation cost		1.4222	1.4334	1.4218	1.4222
Total cost		2.6953	2.5914	2.5856	2.6953

Table 5
Comparison of Calculation of Cases 1–4.

Case No.	Using 2 load curves		Using load curve 2	
	Iterations	Time(h)	Iterations	Time(h)
1	310	43	182	25.5
2	–	–	134	16.9
3	148	12	82	6.55
4	168	4.5	97	2.7

Thus, the smaller gas flow within the pipelines does not exceed the nodal pressure limitations.

The computation times are reported in Table 5. The planning model with two load curves involved nearly twice the computational cost of the planning model with just load curve 2. This is because the planning model with two load curves include twice the number of scenarios compared to the planning model with just load curve 2. More scenarios not only increase the number of iterations to obtain a solution, but also increase the computational time of each iteration. The iterations relating to case 3 were the fewest because this contains the fewest scenarios. Without the Weymouth equation, the variables in case 4 were the fewest, resulting in the fastest computation of each iteration. Case 1 has the most variables and scenarios. Thus, case 1 needed the most iterations to obtain an optimal solution, with the calculation of each iteration taking the longest time.

As basic non-power gas load decreases to 2528.88 kcf/h, case 5 presents the possibility of using just load curve 1. The planning results for case 1 and case 5 using just load curve 1 are shown in Table 6. Here, the wind farm W3 is not installed for there are not enough measures available to accommodate the uncertain wind power. When compared to case 1, the absence of the PtG facilities A1 and A2 to convert excess wind energy into synthetic natural gas, mean that pipelines P1 and P2 have to be constructed to ensure the gas delivery capacity from gas source 1 to the load areas. Gas storage S3, with a large capacity is also installed earlier to balance the temporal fluctuations in gas requirements. The lack of gas also leads to the power output increasing from the coal-fired generators. Transmission lines L15 and L16 have to be built to expand the power transmission ability from the coal-fired generator G8 to the load areas. The installation of PtG therefore directly affects the construction of wind farms and pipelines. The installation of gas storage units and gas-fired generators also needs to consider the synthetic natural gas produced by PtG.

5.2. A Practical Integrated Electricity and Natural Gas System

The proposed approach was also applied to a large-scale IEGS, modified from a real provincial system in Northwestern China, to assess its practicality. The test IEGS consists of a modified 62-bus power system and 25-node natural gas system. The IEGS includes 8 coal-fired and 1 gas-fired generators, 73 lines, 52 electrical loads, 2 gas sources, 21 pipelines, 3 compressor stations and 14 non-power gas loads. The candidate assets include 6 generators (3 being gas), 25 transmission lines, 5 wind farms, 3 PtG facilities, 3 gas storage units and 5 pipelines. The base electrical load and non-power gas load in the first planning year are 11331.92 MW and 3769.5 kcf/h. To make the calculations computationally tractable, 5 incremental segments were adopted. The other parameters were set to be the same as the small-scale IEGS with detailed data provided in [39]. Utilizing the same 5 cases with 2 load curves, the planning results are reported in Table 7.

Case 1: As natural gas in China is scare, the installation of coal-fired generators comes first. Two coal-fired generators, G1 and G6, are built, while only one gas-fired generator, G2, is installed. With rich wind resources, wind farms are expected to generate a great deal of power. Thus, all five wind farms are installed with three PtG facilities converting the excess wind power to synthetic gas. Six lines and five pipelines are installed for energy transmission.

Case 2 is infeasible because of the lack of alternative natural gas storage units to balance the temporal gas demand.

Case 3: If compared to case 1, fewer gas storage units and transmission lines are installed due to the comparatively small amount of wind power in the BS. Without much renewable power, less synthetic gas is produced. So only one gas storage unit, S3, is installed.

Case 4: Without the nodal pressure limitation, the gas transportation ability of pipelines in case 4 is larger than that it is in case 1. Thus, the pipelines in case 4 are installed later and P1 is not installed at all.

Case 5 is infeasible because the gas produced by PtG is an important supplement for the gas supply.

A comparison of cases 1 and 2 is shown in Table 8 based on a high electrical load/low gas load curve. When compared to case 1, a coal-fired generator, G3, is installed to replace the gas-fired generator, G2.

Table 6
Comparison of Cases 1 and 5 with Load Curve 1.

Case	Constructed components
1	$G_{1,1}$,$G_{2,1}$,$G_{3,1}$,$G_{4,4}$,$G_{5,1}$,$G_{6,1}$,$G_{7,2}$,$G_{8,1}$,$W_{1,1}$,$W_{2,1}$,$A_{1,1}$,$A_{2,1}$,$S_{1,1}$,$S_{3,5}$,$S_{4,5}$, $L_{1,1}$,$L_{3,1}$,$L_{4,1}$,$L_{8,1}$,$L_{9,1}$,$L_{11,1}$,$L_{12,2}$,$L_{14,1}$,$P_{3,3}$,$P_{4,4}$,$P_{6,2}$
5	$G_{1,1}$,$G_{2,1}$,$G_{3,1}$,$G_{4,1}$,$G_{5,1}$,$G_{6,4}$,$G_{7,1}$,$G_{8,1}$,$W_{1,1}$,$W_{2,1}$,$S_{1,5}$,$S_{3,2}$,$S_{4,5}$, $L_{1,1}$,$L_{3,2}$,$L_{4,2}$,$L_{8,4}$,$L_{9,1}$,$L_{11,1}$,$L_{12,3}$,$L_{14,2}$,$L_{15,3}$,$L_{16,3}$,$P_{1,5}$,$P_{2,5}$,$P_{3,1}$,$P_{4,4}$,$P_{6,4}$

Table 7
Comparison of Cases 1–5 with Two Load Curves of Large-scale IEGS.

Case	Constructed components
1	$G_{1,3}$,$G_{2,2}$,$G_{6,1}$,$W_{1,1}$,$W_{2,1}$,$W_{3,1}$,$W_{4,1}$,$W_{5,1}$,$A_{1,1}$,$A_{2,1}$,$A_{3,1}$, $S_{1,4}$,$S_{2,5}$,$S_{3,5}$,$L_{1,4}$,$L_{3,1}$,$L_{4,1}$,$L_{5,2}$,$L_{14,1}$,$L_{21,1}$,$P_{1,3}$,$P_{2,3}$,$P_{3,1}$,$P_{4,1}$,$P_{5,1}$
2	Infeasible
3	$G_{1,3}$,$G_{2,2}$,$G_{6,1}$,$W_{1,1}$,$W_{2,1}$,$W_{3,1}$,$W_{4,1}$,$W_{5,1}$,$A_{1,1}$,$A_{2,1}$,$A_{3,1}$,$S_{1,5}$, $L_{1,4}$,$L_{2,2}$,$L_{4,2}$,$L_{14,1}$,$L_{21,1}$,$P_{1,3}$,$P_{2,3}$,$P_{3,1}$,$P_{4,1}$,$P_{5,1}$
4	$G_{1,3}$,$G_{2,2}$,$G_{6,1}$,$W_{1,1}$,$W_{2,1}$,$W_{3,1}$,$W_{4,1}$,$W_{5,1}$,$A_{1,1}$,$A_{2,1}$,$A_{3,1}$, $S_{1,5}$,$S_{2,5}$,$S_{3,5}$,$L_{1,4}$,$L_{3,1}$,$L_{4,1}$,$L_{14,1}$,$L_{2,3}$,$P_{3,2}$,$P_{4,2}$,$P_{5,2}$
5	Infeasible

Table 8
Comparison of Cases 1–2 with Load Curve 1 of Large-scale IEGS.

Case	Constructed components
1	$G_{1,3}$,$G_{2,2}$,$G_{6,1}$,$W_{1,1}$,$W_{2,1}$,$W_{3,1}$,$W_{4,1}$,$W_{5,1}$,$A_{1,1}$,$A_{2,1}$,$A_{3,1}$,$S_{1,5}$,$S_{2,5}$, $L_{1,4}$,$L_{3,1}$,$L_{4,1}$,$L_{5,2}$,$L_{14,1}$,$L_{21,1}$,$P_{1,3}$,$P_{2,3}$,$P_{3,1}$,$P_{4,1}$,$P_{5,1}$
2	$G_{1,1}$,$G_{3,5}$,$G_{6,1}$,$W_{1,1}$,$W_{2,1}$,$W_{3,1}$,$W_{4,1}$,$W_{5,1}$,$A_{1,1}$,$A_{2,1}$,$A_{3,1}$, $L_{1,4}$,$L_{3,1}$,$L_{4,1}$,$L_{14,1}$,$L_{21,1}$,$P_{1,3}$,$P_{2,3}$,$P_{3,1}$,$P_{4,1}$,$P_{5,1}$

Table 9
Comparison of Cases 1 and 5 with Load Curve 1 of Large-scale IEGS.

Case	Constructed components
1	$G_{1,1}$,$G_{2,2}$,$G_{6,1}$,$W_{1,1}$,$W_{2,1}$,$W_{3,1}$,$W_{4,1}$,$W_{5,1}$,$A_{1,1}$,$A_{3,1}$,$S_{1,5}$, $L_{1,4}$,$L_{3,2}$,$L_{4,2}$,$L_{5,5}$,$L_{14,1}$,$L_{21,1}$
5	$G_{1,1}$,$G_{3,3}$,$G_{6,1}$,$W_{1,1}$,$W_{3,3}$,$W_{4,3}$,$W_{5,3}$,$W_{5,1}$,$S_{1,5}$,$S_{3,4}$, $L_{1,4}$,$L_{3,4}$,$L_{4,4}$,$L_{14,2}$,$L_{21,2}$,$P_{1,3}$,$P_{2,3}$,$P_{3,1}$,$P_{4,1}$,$P_{5,1}$

Without gas storages to make up for gaps in the gas supply at peak hours, the gas consumed to generate electricity is reduced to ensure the gas supply for the non-power gas load. Transmission line, L5, is not installed along with G2.

With base non-power gas load decreasing to 2638.65 kcf/h, case 5 is feasible for load curve 1. The planning results of case 1 and case 5 are shown in Table 9.

For case 1, as the non-power gas load decreases, the existing pipelines are sufficient for gas delivery and there is no need for new pipelines. Only the PtG facilities A1 and A3 are built to produce synthetic gas to supplement the gas supply. For now, PtG technology is still not economically attractive due to its high investment and operation costs [5]. Thus, the main rationale for actually constructing a PtG facility is to produce synthetic gas to mitigate potential gas shortages. Comparing case 5 to case 1, the coal-fired generator, G3, replaces the gas-fired generator, G2, to reduce gas consumption. Without PtG, more gas storage units are required to balance the temporal gas demand. Meanwhile, the gas sources have to provide more gas. Pipelines P1-P5 are installed to ensure gas delivery from the gas sources to load areas. The results generated by cases 2 and 5 illustrate that PtG is a promising technology for alleviating natural gas shortages in China. Thus, there is a need for more research to understand how best to apply it in practice.

6. Conclusion

This paper has proposed a coordinated planning model of IEGS that considers the stochasticity of wind power. Not only have coal/gas fired generators, transmission lines, pipelines and wind farms been considered as investment candidates, but also PtG and natural gas storage. The latter play an important part in the planning model by accommodating wind power and balancing temporal energy needs. The stochasticity of wind power was modeled by a limited number of carefully selected scenarios, including ranging from minimum available wind power to maximum available wind power and extreme ramping. IEGS time-series operation were incorporated into the planning model to capture the operational characteristics of natural gas storage and wind power. To make the planning model tractable, the planning model was first reformulated into a large-scale MILP problem with piecewise linearization. Then, a Benders Decomposition based bi-level iterative algorithm was undertaken to obtain the planning solution.

Simulation results have shown that: (1) The uncertainty of wind power has a significant effect on the planning results for an IEGS with wind power. The carefully selected scenarios generated in [34] offer a valid method for modelling the uncertainty of wind power in planning models. (2) Natural gas storage plays an important role in balancing the temporal energy needs of an IEGS. PtG could not only be beneficial for accommodating renewable energy but also provide a vital supplement for natural gas production. PtG, wind farms and natural gas storage together make up a promising combination for alleviating the problems arising from the lack of natural gas in China. (3) Since natural gas storage is able to balance temporal gas demand, it has the potential to influence the installation of gas-fired generators. This, in turn, has an effect upon the installation of transmission lines. (4) As with gas storage, the construction of PtG facility is able to impact the installation of gas-fired generators and transmission lines. In particular, PtG can delay the construction of pipelines. (5) Though a simplified gas flow model makes the planning model more tractable, it may be not precise enough for complicated systems. When simplifying, it is important to consider detailed system parameters. (6) Adopting a time-series-based operational simulation is able to capture the stochasticity of wind power and model gas storage accurately. However, it needs to acknowledged that this accuracy comes at a computational cost.

Declaration of Competing Interest

The authors declare that they have no known competing financial interests or personal relationships that could have appeared to influence the work reported in this paper.

Acknowledgements

This work was supported by National Key Research and Development Program of China (2016YFB0901900) and National Natural Science Foundation of China (51637008).

Appendix A. Supplementary material

Supplementary data to this article can be found online at https://doi.org/10.1016/j.ijepes.2019.105738.

References

[1] Overview and prospect of China's natural gas industry and development in 2016, [Online]. Available: < http://www.chyxx.com/industry/201608/436296.html > .
[2] National Bureau of Statistics of China, National data, Annually Data, [Online]. Available: < http://data.stats.gov.cn/easyquery.htm?cn=C01 > .
[3] Schiebahn S, Grube T, Robinius M, Tietze V, Kumar B, Stolten D. Power-to-gas: technological overview, systems analysis and economic assessment for a case study in Germany. Int J Hydro Energy 2015;40(12):4285–94.
[4] Xing X, Lin J, Song Y, Zhou Y, et al. Modeling and operation of the power-to-gas system for renewables integration: a review. CSEE J Power Energy Syst 2018;4(2):168–78.
[5] Li Y, Liu W, Shahidehpour M, Wen F, Wang K, Huang Y. Optimal operation strategy for integrated natural gas generating unit and power-to-gas conversion facilities.

IEEE Trans Sustain Energy Oct. 2018;9(4):1870–9.
[6] National Development and Refrom Commission, Natural Gas Development "13th five-year plan", [Online]. Available: < http://www.ndrc.gov.cn/fzgggz/fzgh/ghwb/gjjgh/201706/t20170607_850207.html > .
[7] Federal Energy Regulatory Commission (FERC), [Online]. Available: < https://www.ferc.gov/industries/electric/indus-act/electric-coord.asp > .
[8] Australian Energy Market Operator (AEMO), [Online]. Available: < http://www.aemo.com.au/ > .
[9] DRAFT Primer for Gas-Electric Modeling in MISO's Phase III Clean Power Plan Study, [Online]. Available: < https://www.misoenergy.org/ > .
[10] Unsihuay-Vila C, Marangon-Lima JW, Zambroni de Souza AC, et al. A model to long-term, multiarea, multistage, and integrated expansion planning of electricity and natural gas systems. IEEE Trans Power Syst 2010;25(2):1154–68.
[11] Chaudry M, Jenkins N, Qadrdan M, Wu J. Combined gas and electricity network expansion planning. Appl Energy 2014;113:1171–87.
[12] Zhang X, Shahidehpour M, Alabdulwahab AS, Abusorrah A. Security-constrained co-optimization planning of electricity and natural gas transportation infrastructures. IEEE Trans Power Syst 2015;30(6):2984–93.
[13] Nunes JB, Mahmoudi N, Saha TK, Chattopadhyay D. Multi-stage planning framework for electricity and natural gas under high renewable energy penetration. IET Gener Transm Distrib 2018;12(19):4284–91.
[14] Zhao B, Conejo AJ, Sioshansi R. Using electrical energy storage to mitigate natural gas-supply shortages. IEEE Trans Power Syst 2018;33(6):7076–86.
[15] Zhao B, Conejo AJ, Sioshansi R. Coordinated expansion planning of natural gas and electric power systems. IEEE Trans Power Syst 2018;33(3):3064–75.
[16] Qiu J, Yang HM, Dong ZY, Zhao JH, Meng K, Luo FJ, et al. A linear programming approach to expansion planning in gas and electricity markets. IEEE Trans Power Syst 2016;31(5):3594–606.
[17] Correa-Posada CM, Sanchez-Martin P. Gas network optimization: a comparison of piecewise linear models; 2017, [Online]. Available: < http://pdfs.semanticscholar.org/9226/1ed0f303642270fe6b23a71eef30adbcbb43.pdf > .
[18] Zhang Y, Hu Y, Ma J, et al. A mixed-integer linear programming approach to security-constrained co-optimization expansion planning of natural gas and electricity transmission systems. IEEE Trans Power Syst 2018;33(6):6368–78.
[19] Ding T, Hu Y, Bie Z. Multi-stage stochastic programming with nonanticipativity constraints for expansion of combined power and natural gas systems. IEEE Trans Power Syst 2018;33(1):317–28.
[20] He C, Wu L, Liu T, Bie Z. Robust co-optimization planning of interdependent electricity and natural gas systems with a joint N-1 and probabilistic reliability criterion. IEEE Trans Power Syst 2018;33(2):2140–54.
[21] Barati F, Seifi H, Sepasian MS, Nateghi A, Shafie-khah M, Catalão JPS. Multi-period integrated framework of generation, transmission, and natural gas grid expansion planning for large-scale systems. IEEE Trans Power Syst 2015;30(5):2527–37.
[22] Hu Y, Bie Z, Ding T, Lin Y. An NSGA-II based multi-objective optimization for combined gas and electricity network expansion planning. Appl Energy 2016;167(280–293):1.
[23] Zeng Q, Zhang B, Fang J, Chen Z. A bi-level programming for multistage co-expansion planning of the integrated gas and electricity system. Appl Energy 2017;200:192–203.
[24] Qiu J, Dong ZY, Zhao JH, Meng K, Zheng Y, Hill DJ. Low carbon oriented expansion planning of integrated gas and power systems. IEEE Trans Power Syst 2015;30(2):1035–46.
[25] Qiu J, Dong ZY, Zhao JH, Xu Y, Zheng Y, Li CX, et al. Multi-stage flexible expansion planning under uncertainties in a combined electricity and gas market. IEEE Trans Power Syst 2015;30(4):2119–29.
[26] Xiao H, Pei W, Dong Z, Kong L. Bi-level planning for integrated energy systems incorporating demand response and energy storage under uncertain environments using novel metamodel. CSEE J Power Energy Sys. 2018;4(2):155–67.
[27] Odetayo B, Kazemi M, MacCormack J, Rosehart WD, Zareipour H, Seifi AR. A chance constrained programming approach to the integrated planning of electric power generator, natural gas network and storage. IEEE Trans Power Syst Nov. 2018;33(6):6883–93.
[28] Shao C, Shahidehpour M, Wang X, Wang X, Wang B. Integrated planning of electricity and natural gas transportation systems for enhancing the power grid resilience. IEEE Trans Power Syst 2017;32:4418–29.
[29] Dicorato M, Forte G, Pisani M, Trovato M. Planning and operating combined wind-storage system in electricity market. IEEE Trans Sustain Energy 2012;3(2):209–17.
[30] Xiong P, Singh C. Optimal planning of storage in power systems integrated with wind power generator. IEEE Trans Sustain Energy 2016;7(1):232–40.
[31] He Y, Shahidehpour M, Li Z, Guo C, Zhu B. Robust constrained operation of integrated electricity-natural gas system considering distributed natural gas storage. IEEE Trans Sustain Energy 2018;9(3):1061–71.
[32] Clegg S, Mancarella P. Storing renewables in the gas network: modelling of power-to-gas seasonal storage flexibility in low-carbon power systems. IET Gener, Transm Distrib 2016;10(3):566–75.
[33] Bertsimas D, Sim M. The price of robustness. Oper Res 2004;52:35–53.
[34] Zhai Q, Li X, Lei X, Guan X. Transmission constrained UC with wind power: an all-scenario-feasible MILP formulation with strong nonanticipativity. IEEE Trans Power Syst 2017;32(3):1805–17.
[35] Zheng QP, Wang J, Liu AL. Stochastic optimization for unit commitment—a review. IEEE Trans Power Syst 2015;30(4):1–12.
[36] Heitsch H, Römisch W. Scenario reduction algorithms in stochastic programming. Comput Optim Appl 2003;24:187–206.
[37] Chen S, Wei Z, Sun G, Sun Y, Zang H, Zhu Y. Optimal power and gas flow with a limited number of control actions. IEEE Trans Smart Grid 2018;9(5):5371–80.
[38] https://www.dropbox.com/s/tzy98lzbfthjwwc/iegs39-20.xlsx?dl=0.
[39] https://www.dropbox.com/s/fusjo1sr56qe0pz/realiegs.xlsx?dl=0.